EUMETSAT Satellite Application Facility on
Support to Operational Hydrology and Water Management

Algorithm Theoretical Baseline Document (ATBD)
for product H60 P-IN-SEVIRI-PMW, H63 P-IN-SEVIRI-PMW_E

Precipitation rate at ground by GEO/IR
supported by LEO/MW

Reference Number: SAF/HSAF/ATBD-60-63
Issue/Revision Index: 1.0
Last Change: 20 December 2019

1

<div align="center">

DOCUMENT CHANGE RECORD

</div>

Issue / Revision	Date	Description
1.0	20/12/2019	Baseline version prepared for PCR

INDEX

1   Introduction to P-IN-SEVIRI-PMW and P-IN-SEVIRI-PMW_E

1.1   *Principle of the products*

P-IN-SEVIRI-PMW and P-IN-SEVIRI-PMW_E (precipitation rate at ground by GEO/IR supported by LEO/MW) are based on the IR images from the SEVIRI instrument on-board Meteosat Second Generation (MSG) satellites. The spatial coverage of P-IN-SEVIRI-PMW product includes the H SAF area (Europe and Mediterranean basin), Africa and Southern Atlantic Ocean, while the spatial coverage of the P-IN-SEVIRI_E product corresponds to the MSG IODC Full Disk and it includes the Mediterranean basin, Africa, Middle East, and Indian Ocean. Both products are provided on the MSG SEVIRI grid, at the 15-min imaging rate of SEVIRI, and the spatial resolution is consistent with the SEVIRI pixel (3 km^2).

The processing method adopted for both products is called "Rapid Update" (RU). Following this technique, the precipitation estimates are obtained by combining IR GEO equivalent blackbody temperatures (TB) at 10.8 µm with rain rates (RR) from Precipitation Micro-Wave (PMW) measurements. Algorithm is based on a collection of time and space overlapping of both GEO IR imagers and Low Earth Orbit (LEO) PMW sensors (actually SSMIS, AMSU/MHS, AMSR-2, ATMS, and GMI) overpasses. Such a collection consists of a look up table of geolocated relationships rain rate vs TB, updated as soon as new overlapping GEO IR and LEO PMW overpasses (i.e. products P-IN-SSMIS, P-IN-MHS, P-IN-ATMS, H-AUX-17, etc.) are available (Mugnai et al., 2013b, Casella et al., 2013, Sanò et al., 2013, Sanò et al., 2015, Sanò et al., 2016, Casella et al.,2017).

Precipitation estimation of both P-IN-SEVIRI-PMW and P-IN-SEVIRI-PMW_E products is based on the heritage of P-IN-SEVIRI (H03B) rain retrieval and P-IN-SEVIRI-CO (H15B), being the latter specific for convective clouds only. Indeed, H60 production chain identifies convective areas and computes a different RR-TB relationships by distinguish between convective and stratiform clouds (see Sect. 3 for more details). The convective areas are identified with the automatic tool for nowcasting applications NEFODINA (Melfi et al., 2012) explained in Sect. 3.3, which runs at COMet (Centro Operativo per la Meteorologia). It allows the automatic detection and classification of convective cloud systems and the monitoring of their lifecycles. NEFODINA algorithm uses multispectral information from SEVIRI channels at 10.8, 6.2 and 7.3 µm in order to detect and monitor convective processes, and relies on the high temporal repeat cycle of the Meteosat Second Generation (MSG) satellite. Information coming from infrared window at 10.8 µm and water vapour absorption bands (at 6.2 µm and 7.3 µm) is statistically combined in NEFODINA to create an accurate detection-and-tracking procedure for Convective Objects (CO). When a CO is detected, the RU algorithm redistributes precipitation within the rainy MW FOV by concentrating it only in the portion of FOV affected by convection (Antonelli, 2007).

1.2   *Main operational characteristics*

The horizontal resolution (⊔x). The SEVIRI images IFOV is 4.8 km at nadir, and it degrades moving away from nadir, becoming about 8 km over Europe. The sampling distance at the sub-satellite point is ~ 3 km. Conclusion:

• resolution Δx ~ from 4.8 to 8 km - sampling distance: ~ 3 km at the sub-satellite point.

The _observing cycle (Δt)_. It is defined as the average time interval between two measurements over the same area. In the case of P-IN-SEVIRI-PWD the product is generated soon after each SEVIRI new acquisition. Thus:

• observing cycle Δt = 15 min - sampling time: 15 min.

The _timeliness (τ)_.

• timeliness τ ~ 15 min.

The _accuracy_, is evaluated _a-posteriori_ by means of the <u>validation activity</u>.

2 Processing concept

The P-IN-SEVIRI-PMW and P-IN-SEVIRI-PMW_E products are based on MW-derived precipitation estimates from P-IN-SSMIS, P-IN-MHS, P-IN-ATMS, H-AUX-17, H-AUX-20 and on IR images from the SEVIRI sensor on board the geostationary MSG satellites.

SEVIRI is a 12-channel imager observing the Earth–atmosphere system. Eleven channels observe the Earth's full disk with a 15-min repeat cycle. The SEVIRI time and spatial resolutions are thus especially suited for retrieving timely information on rapid weather development and routinely provide instantaneous or cumulated precipitation intensities on time scales consistent with both nature and development of the precipitating cloud systems.

The instantaneous field of view (IFOV) corresponds to the area of sensitivity for each picture element. Since the aperture angle for each IFOV is constant, it follows that the corresponding area at the surface varies with satellite-viewing angle. The image acquisition is based on a constant angular stepping, that is, the subtended angle for each pixel remains constant; hence, the spatial resolution of a pixel at the surface degrades with increasing off-nadir viewing angle.

For the aim of ingesting SEVIRI data into the processing chain of blended algorithm it is necessary to extract from the available image files the information needed by the algorithm. Very briefly, the essential data needed to process SEVIRI image data are:
- the starting and ending date and time of acquisition (UTC) for each image data or area subset;
- the latitude and longitude coordinates for the geo-location of each pixel in the area;
- the Channel 9 (10.8 μm) TB (K) for each pixel. The digital counts are converted into radiances by means of the calibration coefficients distributed along with each image data. Then, radiances are converted into TB by means of a regression relationship and its corresponding coefficients;
- the satellite zenith angle of observation for each pixel (deg);
- the acquisition time of each pixel (or line of pixels) measured in seconds from the starting time of acquisition;
- the nominal line and column number for each pixel.

3   Algorithms description

The following sections describe the principal characteristics of the various software modules that compose both P-IN-SEVIRI-PMW and P-IN-SEVIRI-PMW_E generation chains. The methodology implemented for the ingestion of mandatory input data from both PMW and IR radiometers is the same adopted for P-IN-SEVIRI, apart from the inputs and their format (see Sect. 3.6). However, P-IN-SEVIRI-PMW and P-IN-SEVIRI-PMW_E consider not only P-IN-SSMIS and P-IN-MHS as PMW radiometer data, but also P-IN-ATMS, H-AUX-17, and H-AUX-20. Furthermore, P-IN-SEVIRI-PMW and P-IN-SEVIRI-PMW_E implement different way to calculate stratiform and convective precipitations (see Sect. 3.1).

3.1   Convective and stratiform cases: two different approaches

Rainy pixel of PMW radiometer orbital grid is processed differently depending on whether rainfall is convective or stratiform. The choice of one or the other case depends on the convection file obtained by combining the information deriving from both the NEFODINA SW output (see Sect. 3.3) and the SEVIRI-MSG file containing the Channel 9 (10.8 μm) TB (K). When a PMW radiometer's file is selected, a cycle is performed on the number of pixels, searching the coincidence between TB from IR radiometer and rainfall estimates from PMW radiometer based on both the geographical coordinates and time (see Sect. 3.2).

When the coincidence has been found, firstly, the number of pixels of SEVIRI-MSG belonging to the selected PMW radiometer's one is identified. So, if more than one pixel of the SEVIRI grid has been found, those referring to convective rain are counted (according to the NEFODINA software).

In that case, a factor f is calculated depending on both the overall area of the convective pixels and their number in the following way:

$$f = \frac{N^2}{A}$$

where N is the number of SEVIRI-MSG pixels and A is overall convective area in the PMR radiometer one. Then, f is utilized to correct the PMW radiometer's rainfall estimates, being the latter multiplied by the factor. However, PMW radiometer's estimates are corrected for convective case only if f is greater or equal than 1.

If any TB estimation from SEVIRI-MSG related to the convective case belongs to the considered PMW radiometer's pixel, rainfall estimates from PMW radiometer will be not corrected, and the rain is intended to be stratiform.

3.2   The "Rapid-Update" processing chain

The adopted RU blended technique (Turk et al. 2000 a and b) has been originally developed at the Naval Research Laboratory in Monterey (CA). In the past, the CNR-ISAC adapted the original operational set-up of the software (global, automatic, real time, using a suite of MW and IR observations) to the task of analysing test case studies (Torricella et al. 2007).

Key to the RU blended satellite technique is a real time, underlying collection of time and space overlapping pixels from operational geostationary IR imagers and LEO MW sensors. Rain intensity maps derived from MW measurements are used to create geo-located RR-TB relationships, that are renewed as soon as new co-located data are available from both geostationary and MW instruments.

In the software package these relationships are called histograms. To the aim of evaluate geo-locating histogram relationships, the study area is subdivided in equally spaced lat-lon boxes (2.5° x 2.5°). Histograms are created after the calculation of stratiform and convective precipitations in the PMW radiometer's pixel as described in the previous section.

As soon as new input dataset (MW and IR) is available in the processing chain, the MW-derived RR pixels are paired with their time and space-coincident geostationary 10.8-μm IR TB data, using a 10-minute maximum allowed time offset between the pixel acquisition times and a maximum space offset of 10 km between the pixel coordinates. Each co-located data increments histograms of TB and RR in the nearest 2.5° latitude-longitude box, as well as the eight surrounding boxes (this overlap ensures a fairly smooth transition in the histogram shape between neighbouring boxes). The rationale behind these threshold values for time collocation and box size is discussed by Turk et al. 2002.

In order to set-up a meaningful statistical ensemble, the method can look at older MW-IR slot intersections (no older than 24 h), until a certain (75%) box coverage is reached and a minimum number of coincident observations are gathered for a 2.5° x 2.5° region (at present 400 points, this is a tuneable parameter in the procedure). Thus, RU requires an initial start-up time period (~ 24 h) to allow for establishing meaningful initial relationships all over the study area.

As soon as a box is refreshed with new data, a probabilistic histogram matching relationship (Calheiros and Zawadzki 1987) is updated using the MW RR and IR TB probability distribution functions (PDF), and an updated lookup table (histogram file) is created. The matching is performed as follows:

$$\int_{R_T}^{R_i} p(R)dR = \int_{TB(T)}^{TB(i)} p(T_B)dT_B,$$

where p(R) and p(TB) are the PDF of RR and TB respectively, and R_T and TB(T) are the threshold values. Examples of TB vs RR relationships (histogram) are presented in Fig. 1.
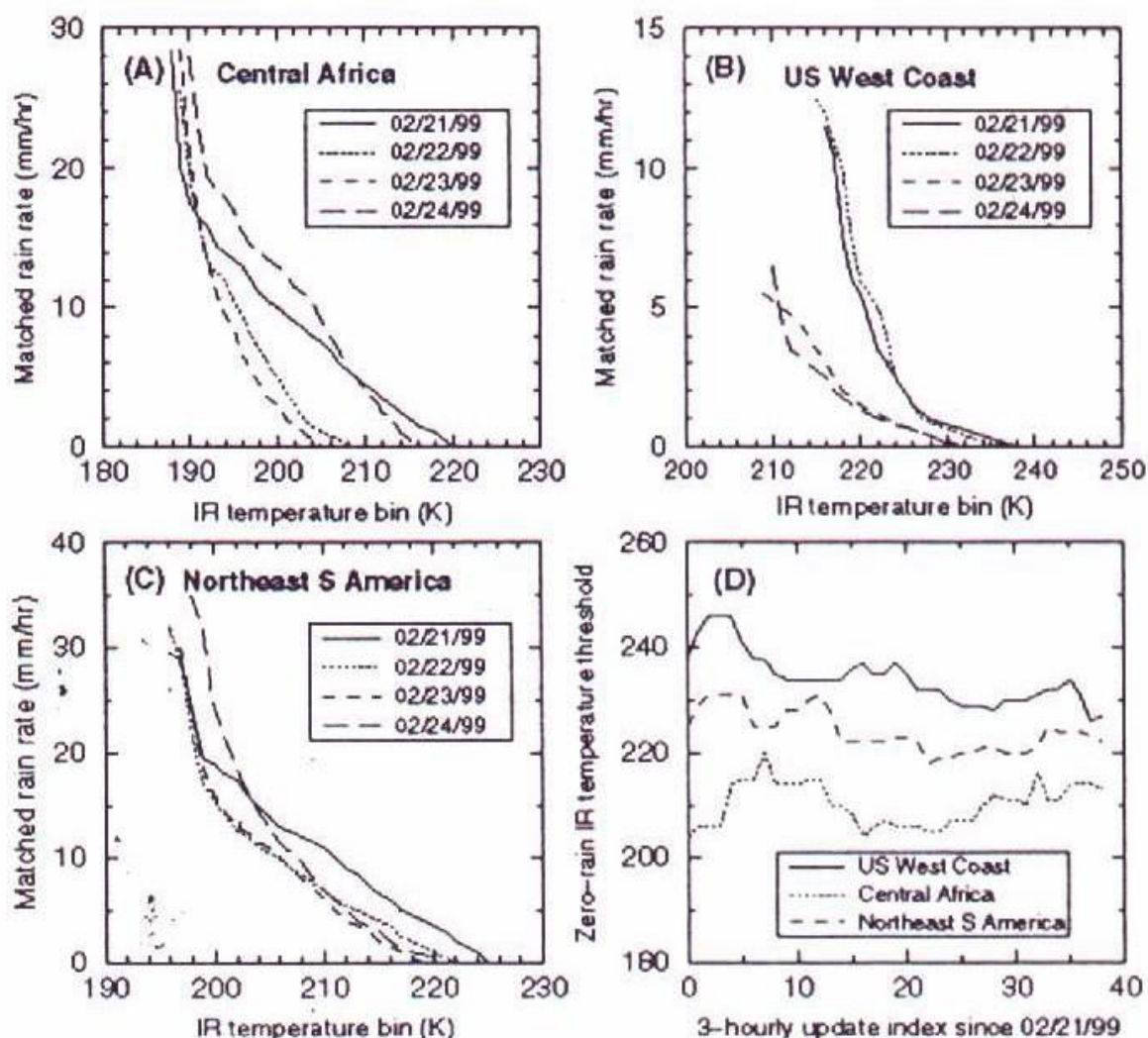
Figure 1: Rain rate vs brightness temperature average relationships for the days and geographical areas marked. (D) presents the zero-rain thresholds as a function of time. Image is taken from Turk et al. (2000a).

The global histograms update process is constantly on-going along with the operational input of MW and geostationary datasets. The transfer of this "background" information to the stream of steadily arriving GEO data involves a computationally fast lookup table and interpolation process for each pixel in the geostationary datasets. For each SEVIRI pixel the RR is finally computed by interpolating the proper TB vs RR histogram, firstly smoothed using the relationships of the surrounding boxes in order to ensure a smooth transition in RR across box boundaries.

If any histogram is more than 24-hours old relative to the IR dataset time, that histogram is not used. In this case a conventional rain rate value = -1 is assigned to each pixel. However, in ordinary operations, the case is only theoretical since, considering the suite of MW data in input to the algorithm, a histogram more recent than 24 hours is nearly always available. In the case of a prolonged interruption of the input data stream (either MW or IR data) the blended product cannot be produced and delivered. Moreover, it will require a start-up period of several hours to restart properly.

3.3   NEFODINA software

NEFODINA SW is an automatic tool for nowcasting applications running at COMET (Melfi et al., 2012). It allows the automatic detection and classification of convective cloud systems and the monitoring of their lifecycles. NEFODINA algorithm uses multispectral information from SEVIRI channels at 10.8, 6.2 and 7.3 μm in order to detect and monitor convective processes and relies on the high temporal repeat cycle of the Meteosat Second Generation (MSG) satellite. Information coming from infrared window at 10.8 μm and water vapour absorption bands (at 6.2μm and 7.3 μm) are statistically combined in NEFODINA to create an accurate detection-and-tracking procedure for Convective Objects (CO). Then NEFODINA moves the attention from pixels to objects (object oriented).

The algorithm classifies and groups neighbouring SEVIRI fields that show convective characteristics. Based on the hypothesis that deep convective clusters are associated with local rapid horizontal variation of cloud volume and WV content, it is possible to classify pixels as convective by detecting temporal variations in cloud top temperatures retrieved in IR at 10.8 μm, and changes in WV content retrieved in the 6.2 μm and at 7.3 μm channels. The IR channel provides cloud top temperature and morphology, while WV channels provide information on the spatial distribution of the WV content in the neighbouring cloud-free area and above the cloud.

NEFODINA produces images of detected cells, their development, and their movement. These output images are associated to quantitative information on the IR, WV1 and WV2 channels BTs along with CO shape, slope index (spatial BT gradient), CO area and CO mean and minimum BTs.

NEFODINA consists of seven main modules:

1.   cloud-cluster detection;
2.   selection of all the potential COs inside the cloud cluster using a varying threshold method in the IR imagery;
3.   continuity test between the objects detected in the last two slots;
4.   discrimination of the objects as already detected or first detections;
5.   calculation of CO parameters in the IR, WV1 and WV2 imagery;
6.   identification of active COs using dynamic thresholds applied to IR, WV1 and WV2 features depending on the parental relationship results;
7.   evaluation of their convective phase.

3.4   Parallax correction algorithm

Once the rain rate has been estimated in each pixel of the SEVIRI grid a methodology to correct the parallax error is applied. Parallax correction is needed to best detect the high cloud top features in satellite imagery having an impact on the satellite-derived products. Parallax effect depends on the cloud top height, the geographical location of the cloud on the ground, and the position of the satellite. Therefore, the higher the cloud, as well as the greater the distance between the zero viewing angle of the satellite point and the cloud position the greater the magnitude of the parallax shift. A schematic illustration of parallax is provided in Fig. 2. The SEVIRI-MSG data are corrected by the parallax shift following the methodology implemented in Radová and Seidl (2008).
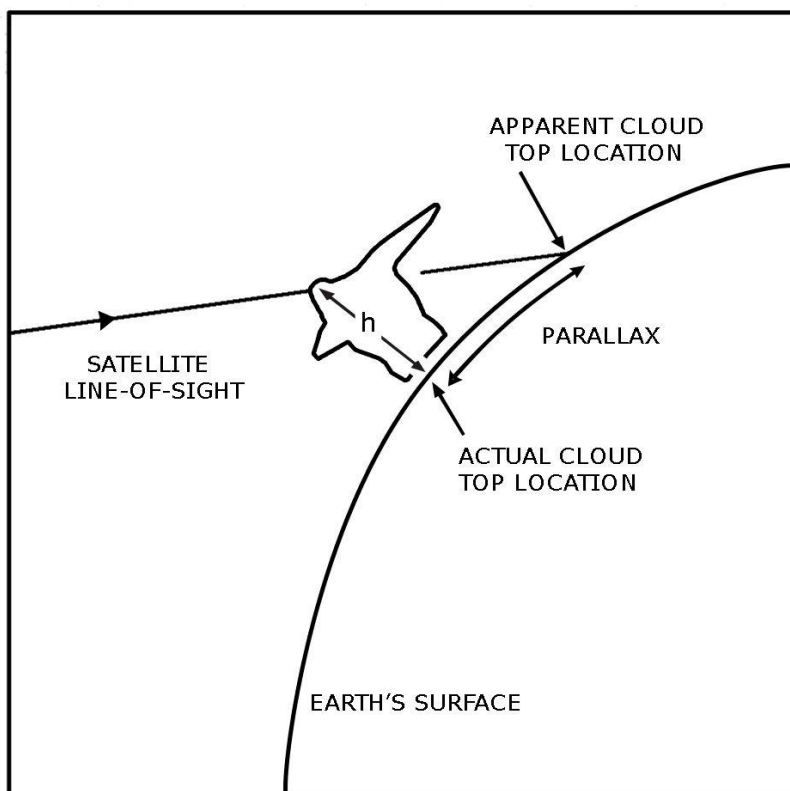
Figure 2: parallax shift concept illustration. Image is taken from Radová and Seidl (2008).

To correct the parallax error the equation of the satellite line-of-sight for a given spot on a cloud top is used. The equation allows to find the apparent position of the spot on the Earth's surface (as seen by the satellite), and it is converted from Cartesian to geodetic coordinates based on a geometric representation of the Earth by a reference ellipsoid (semimajor axis: a = 6378.137 km, semiminor axis: b = 6356.752 km). By means of the geodetic coordinates of the spot it is possible to solve the resulting equation system with respect to geodetic coordinates of the apparent position of the spot, which are finally used to calculate the parallax shift. In this way, the clouds were repositioned by shifting each pixel by a quantity equal to the parallax error. The algorithm processes as input both the RR estimates from PMW radiometer and the cloud top temperature and height (CTTH).

3.5 Quality flag

During the H-SAF Continuous Development Phase-2 (CDOP-2) a quality flag was conceived and associated to the precipitation output of the RU software package with the aim of providing the end-users with a simple and immediate criterion for the evaluation of the product. Two aspects were taken into account for the generation of the quality flag:

1) Quality of the input PMW precipitation products

The P-IN-SEVIRI-PMW product is based on the availability of PMW precipitation estimates used for the calibration of IR brightness. Thus, its quality is linked to the quality of the PMW rainfall estimation input to the algorithms. The PMW quality flags are ingested in terms of percentage values by the RU algorithm and propagated through the code up to the assignment of a quality flag to each TB vs RR relationship (QFmw)

2) Monitoring the PMW precipitation flux timeliness

It is fundamental to monitor the flux of the PMW precipitation products used as inputs, by considering the time difference between the last PMW sensor overpass and the currently processing MSG slot (difftime). This time tells the user how old the calibrations TB vs RR are and thus how adequate they are to be used for the rain rate assignment. An index (QFtime) was modeled to represent the downgrade of the product quality:

$$QF_{time} = exp\left(\frac{-diff_{time}}{time_{limit}}\right) with\, time_{limit} = 5h$$

The total quality flag (QFtotal), which summarizes the two aspects previously described, was generated as follows:

$$QF_{total} = \begin{cases} 0.5 * (QF_{time} + QF_{mw}) & if\, diff_{time} \leq 5h \\ 2/3 * QF_{time} + 1/3 * QF_{mw} & if\, diff_{time} \in]5, 10]h \\ QF_{time} & if\, diff_{time} > 10h \end{cases}$$

3.6 Processing steps overview

This section introduces the main processing steps, which are implemented in both the P-IN-SEVIRI-PMW and P-IN-SEVIRI-PMW_E processing chains.

The processing steps are look like the P-IN-SEVIRI_CO and P-IN-SEVIRI ones. However, P-IN-SEVIRI does not distinguish between convective and stratiform precipitations, whereas in P-IN-SEVIRI-CO processing steps only convective precipitation areas are considered. Instead, convective and stratiform precipitations are calculated in a different way by both P-IN-SEVIRI-PMW and P-IN-SEVIRI-PMW_E (see Sect. 3.1). In particular, they distinguish between convective and stratiform areas by means of NEFODINA SW as well as P-IN-SEVIRI-CO (see Sect. 3.2).

Furthermore, a quality control algorithm is introduced with respect to the pre-existing chains. It performs a final products quality control: output data that are not able to pass this check are not delivered to the users.

Input data comprise both mandatory and auxiliary data. Mandatory data are the SEVIRI-MSG 10.8 μm data giving the TB as well as RR estimates from PMW radiometers. Auxiliary data consist of Cloud Top height (CTTH) product, Cloud Type (CT) from NWC SAF, and NEFODINA .

The SW outputs are:
- RR maps in graphical format (png);
- RR maps encoded in NetCDF;
- log files reporting the quality check status of the operational chain outputs.

The main functions (described in Fig. 3) are:
- ingestion of P-IN-SSMIS, P-IN-MHS, P-IN-ATMS, H-AUX-17, and H-AUX-20 NetCDF format data;
- calculation of TB from 10.8 μm channel masked (from cirrus, broken clouds and semitransparent clouds) by the CT from NWC SAF;
- convection area discrimination by using NEFODINA information;
- association between SEVIRI-MSG TB and MW retrieved precipitation rain rate;
- calculation of the histogram functions in equally spaced lat-lon boxes (2.5° x 2.5°);
- parallax correction by means of NWCSAF CTTH product;
- product quality check (a log file with the check results is provided);

- precipitation rain rate maps, both in graphical (png) and numerical (NetCDF4) formats;

A parallel operational chain with a delay of 3 hours is implemented in order to include the polar MW inputs and to respect the expected timeliness.
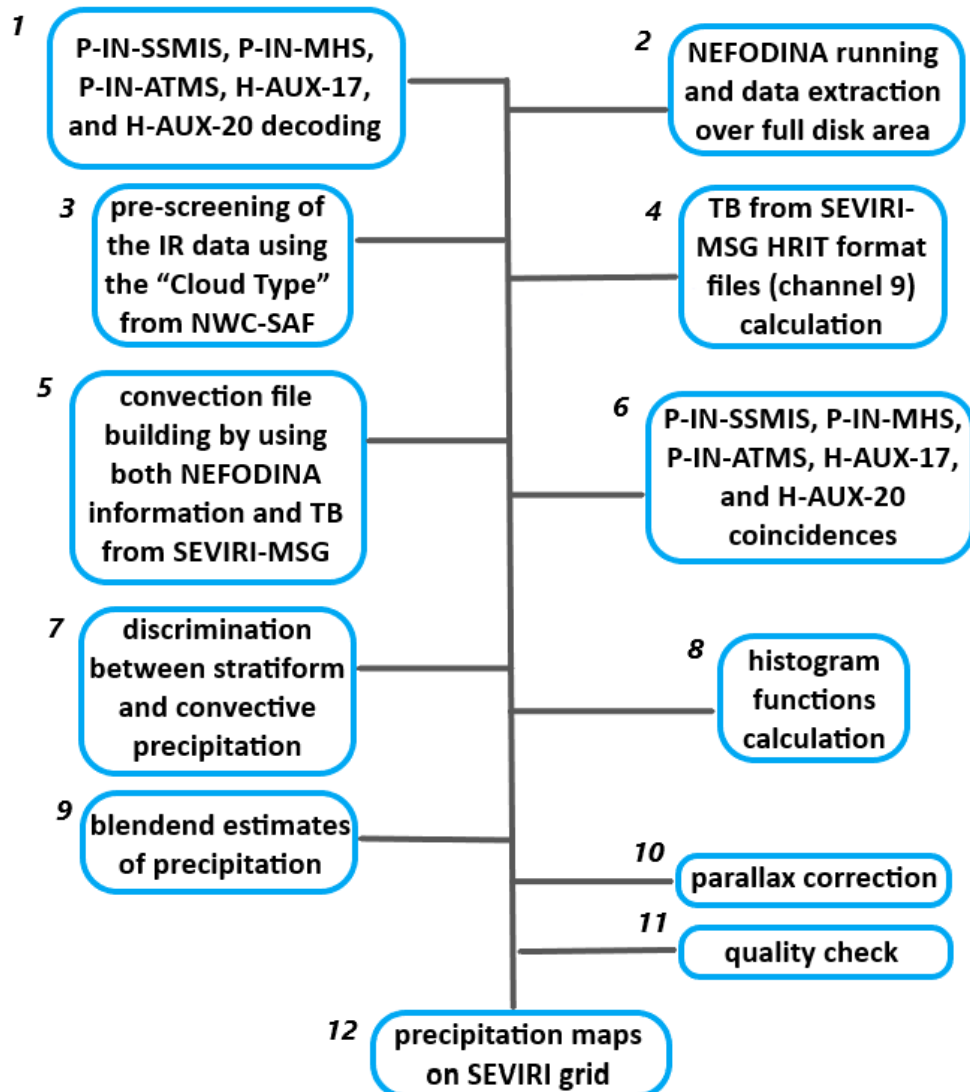
Figure 3: SW package main functions. Blocks have been numbered to allow reading based on the actual processing flow.

Main RU software processing steps are shown in Fig. 4, and detailed in the following:
- pre-processing: preparation and pre-processing of GEO data; preparation and pre-processing of PMW data (from LEO observations);
- co-location: co-located GEO and LEO observations are collected for each lat-lon boxes (2.5° x 2.5°) and accumulated from oldest to newest;
- set-up of geo-located statistical relationships by means of the probability matching technique;
- matching of rain rate to each GEO pixel: production of RR maps at the GEO space-time resolution.

Figure 4: Main processing steps of the RU software package.

4 Validation activities of P-IN-SEVIRI-PMW and P-IN-SEVIRI-PMW_E products

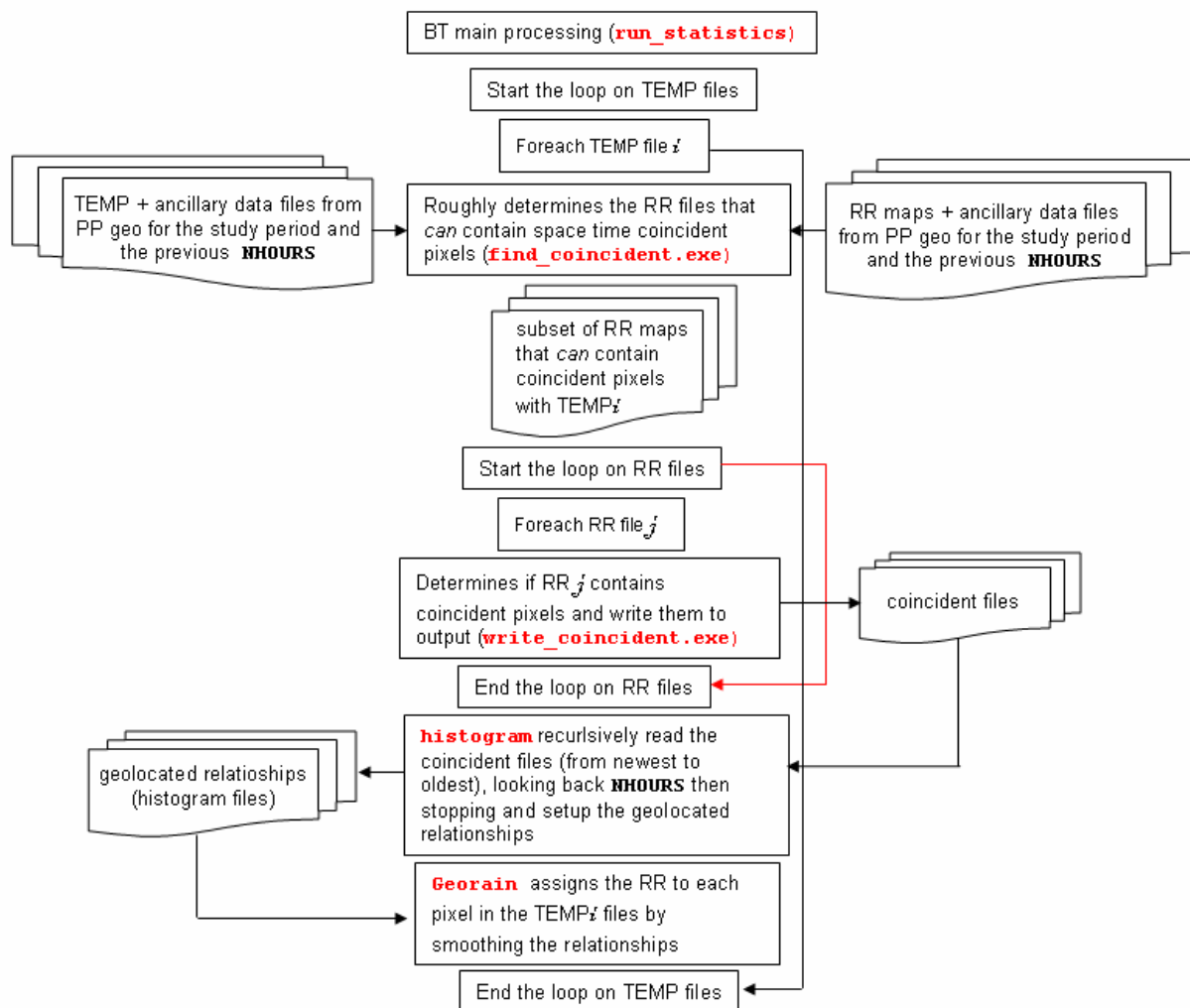The validation methodology of the precipitation products in H-SAF area (European region) is composed by two components: one based on large statistics (multi-categorical and continuous), and one on selected case studies. Both components are considered complementary in assessing the accuracy of the implemented algorithms. Large statistics helps in identifying existence of pathological behaviour, selected case studies are useful in identifying the roots of such behaviour, when present.

During the CDOP-3 the availability of the satellite precipitation products over the full disk poses the problem of their validation outside Europe. In Africa there are few precipitation data derived by ground networks: the operational raingauges stations are sparse and the radar networks are often not fully operational or not available at all. For all these reasons the large statistic quality assessment in African region will be mainly focused on the comparison of H-SAF precipitation products with other satellite products as the Global Precipitation Mission (GPM) products derived by Dual-frequency (Ka-band and Ku-band) Precipitation Radar (DPR). An associate scientist activity (Sebastianelli, 2017) has

been established that the most suitable GPM-DPR products for the validation activity are the dual-frequency ones.

The RU algorithm is also subject to a continuous effort of validation and intercomparison in different validation sites all over the world within the International Precipitation Working Group (IPWG) activities, in particular Fig. 5 shows an examples of validation outputs over Japan. The description of the operational set-up of the RU being validated and up-to-date results of the validation activity are available at the IPWG web site at http://www.isac.cnr.it/~ipwg .

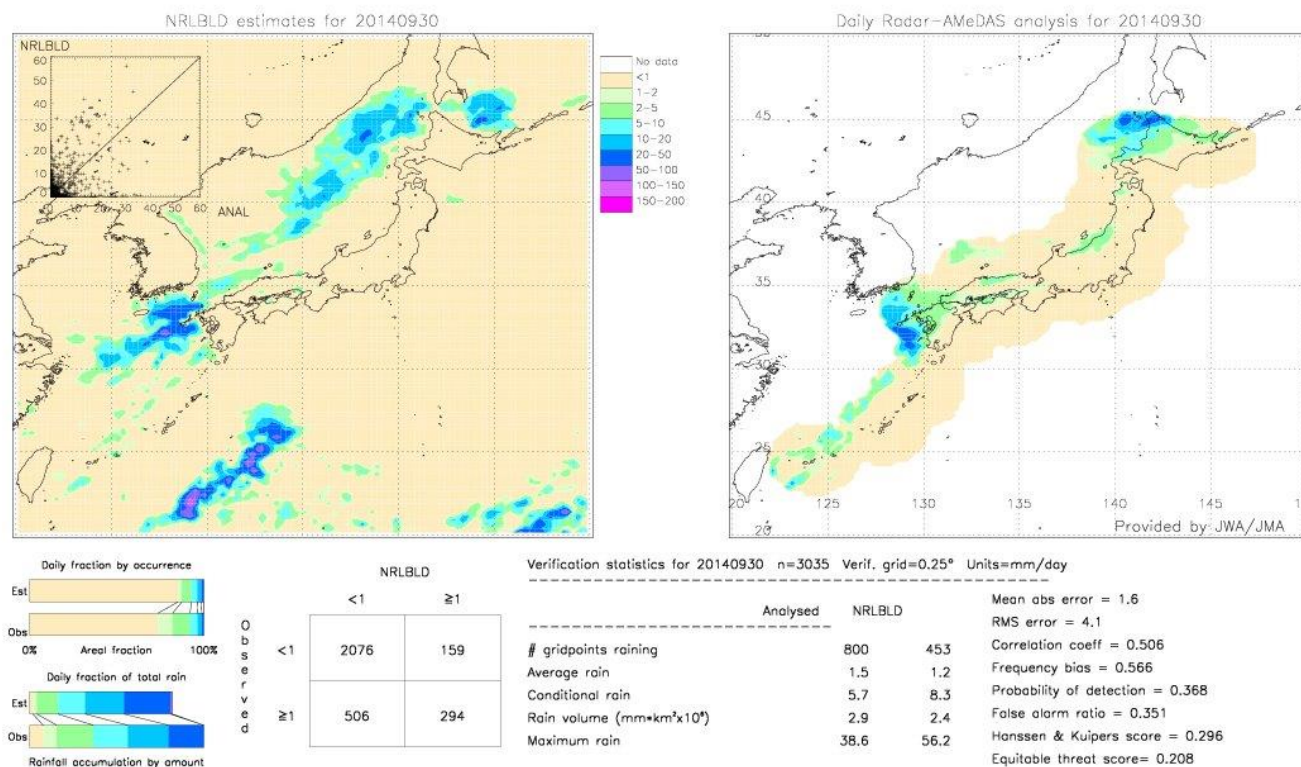**Figure 5. Example of IPWG validation results over Japan, 30 September 2014.**

5 Examples of P-IN-SEVIRI-PMW product

Currently, P-IN-SEVIRI-PMW is not yet generated on a regular basis. A prototype example is provided in Fig. 6. The spatial coverage of the product is 60°S – 75°N, 80°W – 80°E.
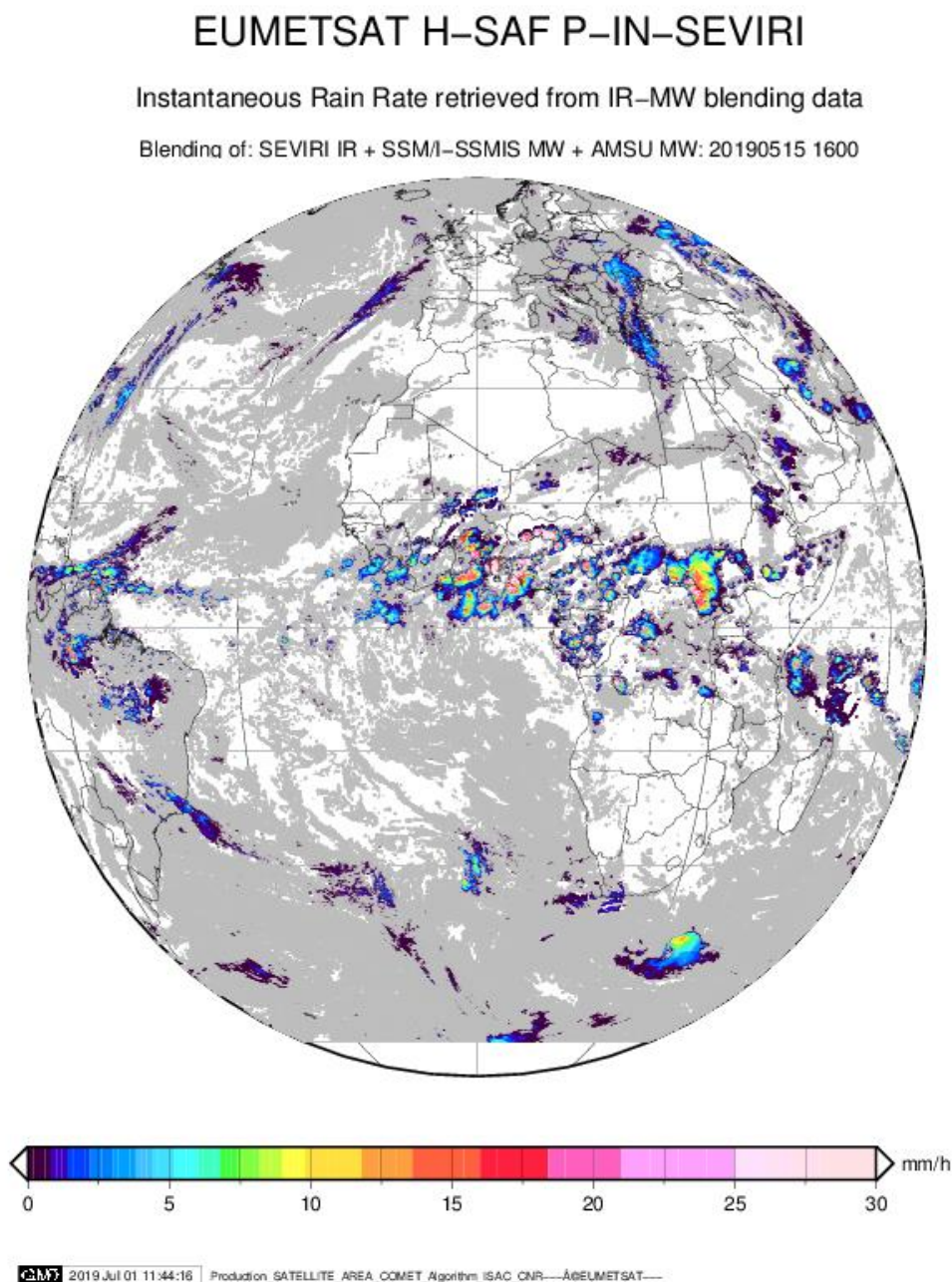

Figure 6: prototype example of the P-IN-SEVIRI-PMW product relative to the May 5, 201922:30 UTC.

6 Applicable documents

1- CDOP3 PRD – H-SAF CDOP3 Product Requirement Document Rel. 1.2,
Ref: SAF/HSAF/CDOP3/PRD/1.2

7 References

Antonelli P. 2007:" Refinement and operational implementation of a rain rate algorithm based on AMSU/MHS and rain gauge data over H-SAF area".

Calheiros R.V. and I. Zawadzki, 1987: "Reflectivity rain-rate relationship for radar hydrology and Brazil". J. Clim. Appl. Meteor., 26, 118-132.

Cappelaere, B., Descroix, L., Lebel, T., Boulain, N., Ramier, D., Laurent, J. P., Favreau, G., Boubkraoui, S., Boucher, M., Moussa, I. B., Chaffard, V., Hiernaux, P., Issoufou, H. B. A., LeBreton, E., Mamadou, I., Nazoumou, Y., Oi, M., Ottle, C., & Quantin, G. (2009). The AMMA- CATCH experiment in the cultivated Sahelian area of south-west Niger- Investigating water cycle response to a fluctuating climate and changing environment. Journal of Hydrology, 375, 34-51;

Doumounia, A, M Gosset, F Cazenave, M Kacouand F Zougmore, 2014; Rainfall Monitoring based on Microwave links from cellular telecommunication Networks: First Results from a West African Test Bed. Geophysical Research Letters, 10. 1002/2014GL060724;

Gosset M, E. P. Zahiriand S Moumouni, 2010: Rain Drop Size distributions variability and impact on X---band polarimetric radar retrieval: results from the AMMA campaign in Benin. Quarterly Journal of the Royal Meteorological Society, 136, 243---256. DOI:10. 1002/qj. 556.

Gosset Marielle, Viarre J., Quantin G., Alcoba M., 2013. Evaluation of several rainfall; products used for hydrological applications over West Africa using two high---resolution gauge networks. Quarterly Journal of the Royal Meteorological Society, 2013, 139 (673), p. 923---940. ISSN0035---9009;doi:10. 1002/qj. 2130;

Koffi, A. K., M. Gosset, E. ---P. Zahiri, A. D. Ochou, M. Kacou, F. Cazenave, andP. Assamoi, 2014: Evaluation of X-band polarimetric radar estimation of rainfall and rain drop size distribution parameters in West Africa. Atmos. Res., 143, 438–4doi:10. 1016/j. atmos res. 2014. 03. 009;

Panthou, G., Vischel, T. and Lebel, T., 2014: Recent trends in the regime of extreme rainfall in the Central Sahel. International Journal of Climatology, 34, 3998-4006;

Puca, S., F. Porcù, A. Rinollo, G. Vulpiani, P. Baguis, S. Balabanova, E. Campione, A. Ertürk, S. Gabellani, R. Iwanski, M. Jurašek, J. Kanák, J. Kerényi, G. Koshinchanov, G. Kozinarova, P. Krahe, B. Łapeta, E. Lábó, L. Milani, L'. Okon, A. Öztopal, P. Pagliara, F. Pignone, C. Rachimow, N. Rebora, E. Roulin, I. Sönmez, A. Toniazzo, D. Biron, D. Casella, E. Cattani, S. Dietrich, F. Di Paola, S. Laviola, V. Levizzani, D. Melfi, A. Mugnai, G. Panegrossi, M. Petracca, P. Sanò, F. Zauli, P. Rosci, L. De Leonibus, E. Agosta, F. Gattari, The validation service of the hydrological SAF geostationary and polar satellite precipitation products, Nat. Hazards Earth Syst. Sci., 14, 871–889, 2014;

Radová, Michaela, and Jakub Seidl. "Parallax applications when comparing radar and satellite data." The 2008 EUMETSAT Meteorological Satellite Conference (conference proceedings). 2008.

Schmetz J., P. Pili, S. Tjemkes, D. Just, J. Kerkmann, S. Rota and A. Ratier, 2002: "An introduction to METEOSAT Second Generation (MSG)". Bull. Amer. Meteor. Soc., 83, 977-992.

Sebastianelli, S.: "Potentials and limitations of the use of GPM-DPR for validation of H-SAF precipitation products: study over the italian territory". Final report of associate scientist activity REF. HSAF_AS16_03.

Torricella F., V. Levizzani and F.J. Turk, 2007: "Application of a blended MW-IR rainfall algorithm to the Mediterranean". In: Measuring precipitation from space – EURAINSAT and the future. V. Levizzani, P. Bauer, and F. J. Turk, Eds., Springer, 497-507.

Turk F.J., E.E. Ebert, B.-J. Sohn, H.-J. Oh, V. Levizzani, E.A. Smith and R.R. Ferraro, 2002: "Validation of an operational global precipitation analysis at short time scales". Proc. 1st IPWG Workshop, Madrid, 23-27 Sept., 225-248.

Turk J.F., G. Rohaly, J. Hawkins, E.A. Smith, F.S. Marzano, A. Mugnai and V. Levizzani, 2000a: "Meteorological applications of precipitation estimation from combined SSM/I, TRMM and geostationary satellite data". Microwave Radiometry and Remote Sensing of the Earth's Surface and Atmosphere, P. Pampaloni and S. Paloscia Eds., VSP Int. Sci. Publisher, Utrecht (The Netherlands), 353-363.

Turk J.F., G. Rohaly, J. Hawkins, E.A. Smith, F.S. Marzano, A. Mugnai and V. Levizzani, 2000b: "Analysis and assimilation of rainfall from blended SSMI, TRMM and geostationary satellite data". Proc. 10th AMS Conf. Sat. Meteor. and Ocean., 9, 66-69.

Turk J.F., B.-J. Sohn, H.-J. Oh, E.E. Ebert, V. Levizzani, and E.A. Smith, 2009: "Validating a rapid update satellite precipitation analysis across telescoping space and time scales". Meteor. Atmos. Phys., 105, 99-108.

Vischel T., Quantin G., Lebel Thierry, Viarre J., Gosset Marielle, Cazenave Frédéric, Panthou G. Generation of high-resolution rain fields in west Africa: evaluation of dynamic interpolation methods. Journal of Hydrometeorology, 2011, 12(6), p. 1465-1482. ISSN 1525-755X.

Annex 1: Acronyms

AMSU	Advanced Microwave Sounding Unit (on NOAA and MetOp)
AMSU-A	Advanced Microwave Sounding Unit - A (on NOAA and MetOp)
AMSU-B	Advanced Microwave Sounding Unit - B (on NOAA up to 17)
ATDD	Algorithms Theoretical Definition Document
AU	Anadolu University (in Turkey)
BfG	Bundesanstalt für Gewässerkunde (in Germany)
CAF	Central Application Facility (of EUMETSAT)
CDOP	Continuous Development-Operations Phase
CESBIO	Centre d'Etudes Spatiales de la BIOsphere (of CNRS, in France)
CM-SAF	SAF on Climate Monitoring
COMet	Centro Operativo per la Meteorologia (in Italy)
CNR	Consiglio Nazionale delle Ricerche (of Italy)
CNRS	Centre Nationale de la Recherche Scientifique (of France)
DMSP	Defense Meteorological Satellite Program
DPC	Dipartimento Protezione Civile (of Italy)
EARS	EUMETSAT Advanced Retransmission Service
ECMWF	European Centre for Medium-range Weather Forecasts
EDC	EUMETSAT Data Centre, previously known as U-MARF
EUM	Short for EUMETSAT
EUMETCast	EUMETSAT's Broadcast System for Environmental Data
EUMETSAT	European Organisation for the Exploitation of Meteorological Satellites
FMI	Finnish Meteorological Institute
FTP	File Transfer Protocol
GEO	Geostationary Earth Orbit
HDF	Hierarchical Data Format
HRV	High Resolution Visible (one SEVIRI channel)
H-SAF	SAF on Support to Operational Hydrology and Water Management
IDL©	Interactive Data Language
IFOV	Instantaneous Field Of View
IMWM	Institute of Meteorology and Water Management (in Poland)
IPF	Institut für Photogrammetrie und Fernerkundung (of TU-Wien, in Austria), now Department of Geodesy and Geoinformation
IPWG	International Precipitation Working Group
IR	Infra Red
IRM	Institut Royal Météorologique (of Belgium) (alternative of RMI)
ISAC	Istituto di Scienze dell'Atmosfera e del Clima (of CNR, Italy)
ITU	İstanbul Technical University (in Turkey)
LATMOS	Laboratoire Atmosphères, Milieux, Observations Spatiales (of CNRS, in France)
LEO	Low Earth Orbit
LSA-SAF	SAF on Land Surface Analysis
Météo France	National Meteorological Service of France
METU	Middle East Technical University (in Turkey)
MHS	Microwave Humidity Sounder (on NOAA 18 and 19, and on MetOp)
MSG	Meteosat Second Generation (Meteosat 8, 9, 10, 11)
MVIRI	Meteosat Visible and Infra Red Imager (on Meteosat up to 7)
MW	Micro Wave
NESDIS	National Environmental Satellite, Data and Information Services
NMA	National Meteorological Administration (of Romania)
NOAA	National Oceanic and Atmospheric Administration (Agency and satellite)
NRT	Near real-time
NWC-SAF	SAF in support to Nowcasting & Very Short Range Forecasting
NWP	Numerical Weather Prediction
NWP-SAF	SAF on Numerical Weather Prediction
O3M-SAF	SAF on Ozone and Atmospheric Chemistry Monitoring
OMSZ	Hungarian Meteorological Service
ORR	Operations Readiness Review

18

OSI-SAF	SAF on Ocean and Sea Ice
PDF	Probability Density Function
PEHRPP	Pilot Evaluation of High Resolution Precipitation Products
Pixel	Picture element
PMW	Passive Micro-Wave
PP	Project Plan
PPF	Product Processing Facility
PR	Precipitation Radar (on TRMM)
PUM	Product User Manual
PVR	Product Validation Report
REMet	Reparto di Meteorologia (in Italy)
RMI	Royal Meteorological Institute (of Belgium) (alternative of IRM)
RR	Rain Rate
RU	Rapid Update
SAF	Satellite Application Facility
SEVIRI	Spinning Enhanced Visible and Infra-Red Imager (on Meteosat from 8 onwards)
SHMÚ	Slovak Hydro-Meteorological Institute
SSM/I	Special Sensor Microwave / Imager (on DMSP up to F-15)
SSMIS	Special Sensor Microwave Imager/Sounder (on DMSP starting with S-16)
SYKE	Suomen ympäristökeskus (Finnish Environment Institute)
TB	Equivalent Blackbody Temperature (used for IR)
TKK	Teknillinen korkeakoulu (Helsinki University of Technology)
TMI	TRMM Microwave Imager (on TRMM)
TRMM	Tropical Rainfall Measuring Mission
TSMS	Turkish State Meteorological Service
TU-Wien	Technische Universität Wien (in Austria)
U-MARF	Unified Meteorological Archive and Retrieval Facility
UniFe	University of Ferrara (in Italy)
URD	User Requirements Document
UTC	Universal Coordinated Time
VIS	Visible
ZAMG	Zentralanstalt für Meteorologie und Geodynamik (of Austria)